JOURNAL OF SOLID STATE CHEMISTRY **126,** 328–335 (1996)
ARTICLE NO. 0345

Crystal Structure and Characterization of $Ba_2V_3O_9$: A Vanadyl(IV) Vanadate Containing Rutile-like Chains of VO_6 Octahedra

Anne-Claire Dhaussy and Francis Abraham[1]

Laboratoire de Cristallochimie et Physicochimie du Solide, URA CNRS 452, ENSCL, Université des Sciences et Technologies de Lille, BP 108, 59652 Villeneuve d'Ascq Cedex, France

and

Olivier Mentre[2] and Hugo Steinfink

Center of Materials Science & Engineering, University of Texas at Austin, E.T.C 9.108, Austin, Texas 78712-1062

Received June 17, 1996; in revised form August 5, 1996; accepted August 7, 1996

The crystal structure of $Ba_2V_3O_9$ has been determined and refined to final R and R_w values of 0.025 and 0.028 from 1562 independent single crystal reflections. It crystallizes in the space group $P2_1/m$ with $a = 9.302(1)$ Å, $b = 5.969(1)$ Å, $c = 8.118(1)$ Å, and $\beta = 113.96(1)°$. The structure consists of one-dimensional rutile-type chains of edge-sharing VO_6 octahedra parallel to the b axis. The VO_4 tetrahedra share corners with VO_6 octahedra of a single rutile-type chain to form one-dimensional $[V_3O_9]^{4-}_{\infty}$ columns which are held together by Ba^{2+} ions. In this mixed valence compound V^{4+} and V^{5+} ions are distributed in an ordered way in octahedra and tetrahedra, respectively. In the almost perfect O_6 octahedron the vanadium atom is off-center so that it forms a short vanadyl V=O bond of 1.686(3) Å, typical of a V^{4+} ion. This compound is a barium vanadyl vanadate $Ba_2(VO)(VO_4)_2$. It is the first example of isolated rutile-type chains found with V^{4+} ions. Magnetic susceptibility measurements show that this phase is an antiferromagnet with $T_N \cong 58$ K. At about 20 K magnetic anisotropy causes a canted spin arrangement.

INTRODUCTION

Mixed valence vanadium compounds are important in solid state chemistry because the many oxidation states lead to a variety of crystal structures and nonstoichiometric phases. They exhibit complex magnetic and electrical properties. Recently Mentre and Abraham (1) discovered two new compounds in the Pb–V–O system, $Pb_{1.32}V_{8.35}O_{16.7}$ and PbV_6O_{11}. The former adopts a hollandite-related structure with lead atoms and VO_4 tetrahedra occupying the large tunnels of the V_8O_{16} hollandite framework. The structure of the latter is closely related to that of AV_6O_{11} compounds (A = Na, Sr) which crystallize with an R-type hexagonal ferrite structure (2–4). A solid solution phase $BaV_{10-x}O_{17}$ ($0.10 \leq x \leq 0.65$) has been described that also displays a modified hollandite structure whose tunnels accommodate alternately Ba and O atoms. The tunnel O atoms generate octahedral sites which are statistically occupied by V atoms, thus causing the wide solid-solution range (5). Bouloux *et al.* (6) have reported a hollandite-type phase $Ba_xV_8O_{16}$, ($1.20 \leq x \leq 1.36$), and very recently Kanke *et al.* (7) refined the crystal structure of the tetragonal priderite-type compound $Ba_{1.09}V_8O_{16}$. These phases contain both trivalent and tetravalent vanadium cations. The recently described $Ba_8V_7O_{22}$ is the first example of a vandium oxide phase in which all three oxidation states of vanadium, V^{3+}, V^{4+}, and V^{5+}, coexist (8). Although barium trivalent or tetravalent vanadyl phosphates and arsenates have been described (9–15), no barium vanadyl(IV) vanadate has been characterized to date.

During our attempts to prepare barium mixed-valence vanadium oxides, single crystals whose composition corresponded to $Ba_2V_3O_9$ were often obtained. This compound was first synthesized by Bouloux *et al.* (6) and was shown to crystallize in the monoclinic system, but its crystal structure was not determined. The chemical composition seems to indicate the presence of V^{4+} and V^{5+} and we undertook a single crystal X-ray diffraction structure determination as well as magnetic and IR studies. The results of these experiments show that indeed the compound is a barium vanadyl(IV) vanadate, $Ba_2(VO)(VO_4)_2$.

[1] To whom correspondence should be addressed.

[2] Permanent address: Laboratoire de Cristallochimie et Physicochimie du Solide, Ecole Nationale Supérieure de Chimie de Lille, B.P.108, 59652 Villeneuve d'Ascq.

0022-4596/96 $18.00

EXPERIMENTAL

Synthesis

$Ba_2V_2O_7$ was obtained by heating a mixture of $BaCO_3$ (Aldrich 98%) and V_2O_5 (Aldrich 99.6%) in a 2:1 molar ratio at 750°C for 5 days. V_2O_3 was obtained by reducing V_2O_5 in hydrogen at 850°C. Bouloux *et al.* (6) prepared $Ba_2V_3O_9$ by solid state reaction between $Ba_2V_2O_7$ and VO_2. In our experiments VO_2 was prepared *in situ,* thus $Ba_2V_2O_7$, V_2O_5, and V_2O_3 were mixed in a 4:1:1 molar ratio. About 0.3 g of the mixture was introduced into a gold tube, sealed in an evacuated silica tube, and then heated at 900°C for 48 h. Regrinding and reheating was needed to achieve a single phase product as evidenced by the match of the powder X-ray diffraction pattern with that reported for $Ba_2V_3O_9$ (16).

Single crystals were obtained from the same mixture heated at 1010°C, cooled at 4°C/h to 850°C, and then furnace cooled. Red, acicular, crystals were obtained. Bouloux *et al.* (6) reported the lattice parameters and space group from Weissenberg photographs and indexed the X-ray diffraction powder data using a nonstandard, *B*-centered monoclinic cell with $a = 8.108(6)$ Å, $b = 5.970(4)$ Å, $c = 17.02(1)$ Å, and $\beta = 91.96(10)°$. We transformed to a primitive cell and the lattice parameters reported in Table 1 resulted from a least-squares refinement of an indexed powder X-ray diffraction pattern obtained with a Siemens D5000 diffractometer equipped with a graphite crystal diffracted-beam monochromator and Cu$K\alpha$ radiation.

Single Crystal X-Ray Analysis

Preliminary Weissenberg photographs confirmed the $2/m$ diffraction symmetry. The data collection parameters are reported in Table 1. Intensities were corrected for Lorentz-polarization effects. Absorption corrections were applied using the analytical method of De Meulenaer and Tompa (17). The density was determined with a AccuPyc 1330 He gas displacement pycnometer. The systematic absences $k = 2n + l$ for $0k0$ are consistent with space groups $P2_1$ (No. 4) and $P2_1/m$ (No. 11). The structure was successfully solved and refined in $P2_1/m$. The coordinates of the barium atoms were determined from a three dimensional Patterson synthesis. Difference Fourier syntheses calculated at subsequent stages located the vanadium and oxygen atoms. Atom V(3) was statistically distributed over its crystallographic site. The refinement of the coordinates and the anisotropic displacement parameters shown in Tables 2 and 3 converged to $R = 0.025$, $R_w = 0.028$, Table 1. Values of the scattering factors for neutral atoms were obtained from (18) and the anomalous dispersion corrections from Cromer and Liberman (19). The full matrix least squares refinements were performed with a local modification of SFLS-5 (20). A table of F_o, F_c, and $\sigma(F_o)$ has been deposited.[3]

TABLE 1
Crystal Data, Intensity Measurement, and Structure Refinement Parameters for $Ba_2V_3O_9$

Crystal data	
Crystal symmetry	Monoclinic
Space group	$P2_1/m$
Cell dimension (Å)	
a, (Å)	9.302(1),
b, (Å)	5.969(1),
c, (Å)	8.118(1),
β, (°)	113.96(1)
Volume, Å^3	411.893
Density calc., g · cm^{-3}	4.61
Density mes., g · cm^{-3}	4.65(3)
Z	2
Data collection	
Equipment	Philips PW 1100
λMo$K\alpha$ (graphite monochromator)	0.7107 Å
Scan mode	$\omega - 2\theta$
Scan width	1.2°
θ range	2–35°
Standard reflections measured every 2 hours (no decay)	$10\bar{2}$, $21\bar{2}$, 211
Recording reciprocal space	$-15 \le h \le 15$, $-9 \le k \le 9$, $0 \le l \le 13$
Number of measured reflections	3817
Number of reflections $I > 3\sigma(I)$	2955
Number of independent reflections	1562
μ, cm^{-1}	132
Limiting faces and distances (mm) from arbitrary origin	100 0.010 $\bar{1}00$ 0.010 010 0.200 $0\bar{1}0$ 0.200 001 0.015 $00\bar{1}$ 0.015
Transmission factor range	0.61–0.79
Merging R factor	0.018
Refinement	
Number of refined parameters	83
$R = \Sigma\|\|F_o\| - \|F_c\|\|/\Sigma F_o$	0.025
$R_w = [\Sigma w(F_o - F_c)^2/\Sigma w F_o^2]^{1/2}$	0.028
$w = 1/\sigma(F_o)$	

Infrared and Magnetic Measurements

Infrared data for $Ba_2V_3O_9$ were collected on a Nicolet-Magna 750 Fourier transformed IR spectrometer. Mag-

[3] See NAPS document No. 05338 for 18 pages of supplementary material. This is not a multi-article document. Order from ASIS/NAPS Microfiche Publications, P. O. Box 3513, Grand Central Station, New York, NY 10163-3513. Remit in advance $4.00 for microfiche copy or for photocopy, $7.75 up to 20 pages plus $.30 for each additional page. All orders must be prepaid. Institutions and organizations may order by purchase order. However there is a billing and handling charge for this service of $15. Foreign orders add $4.50 for postage and handling, for the first 20 pages, and $1.00 for additional 10 pages of material, $1.50 for postage of any microfiche orders.

TABLE 2
Atomic Positions, Occupancies, Positional Parameters, and Equivalent Isotropic Displacement Parameters, Å²

Atom	Site	Occ.	*x*	*y*	*z*	B_{eq} (Å²)[a]
Ba(1)	2*e*	1	0.58821(3)	1/4	0.19377(4)	0.72(1)
Ba(2)	2*e*	1	0.76547(3)	1/4	0.78224(4)	1.22(1)
V(1)	2*e*	1	0.32357(8)	1/4	0.52905(10)	0.57(1)
V(2)	2*e*	1	0.18540(9)	1/4	−0.07637(10)	0.62(1)
V(3)	4*f*	0.5	0.98928(16)	0.03453(18)	0.47520(16)	0.53(3)
O(1)	4*f*	1	0.3047(3)	0.0236(4)	−0.0083(3)	1.06(6)
O(2)	4*f*	1	0.2088(3)	0.0050(4)	0.4918(3)	0.88(5)
O(3)	2*e*	1	0.4228(6)	1/4	0.3991(6)	2.10(12)
O(4)	2*e*	1	0.0681(5)	1/4	0.0310(6)	2.23(12)
O(5)	2*e*	1	0.4537(4)	1/4	0.7435(5)	1.28(8)
O(6)	2*e*	1	0.9283(4)	1/4	0.3286(5)	0.85(7)
O(7)	2*e*	1	0.0618(4)	1/4	−0.3210(4)	0.76(7)

[a] B_{eq} is defined by $B_{eq} = 4/3\ \Sigma_i\Sigma_j\beta_{ij}a_ia_j$.

netic susceptibilities were measured with a Quantum Design DC SQUID magnetometer over the range 10–300 K for zero-field-cooled (ZFC) samples and over the range 300–10 K for field-cooled (FC) samples. The measurements for ZFC were taken by equilibrating the sample at 10 K, switching on a magnetic field of 3 kOe, and recording the magnetization as a function of temperature to 300 K. With the applied field on, measurements of susceptibility were then continued while the sample was cooled from 300 to 10 K to obtain FC data.

DISCUSSION

Selected bond distances and bond angles are given in Table 4. A projection of the structure along the *b* axis is shown in Fig. 1. V(1) and V(2) are tetrahedrally coordinated to oxygen and V(3) is in an octahedral environment. The $V(3)O_6$ octahedra form linear, rutile-type, edge-sharing chains parallel to **b**. The $V(1)O_4$ and $V(2)O_4$ tetrahedra share corners with the $[V(3)O_4]_\infty$ chains to constitute infinite, one-dimensional columns of the formula $[V_3O_9]_\infty^{4-}$, (Fig. 2). The columns are held together by Ba ions.

Rutile chains are found both in low-temperature and high-temperature forms of vanadium dioxide. In the tetragonal high-temperature form the six V–O distances are nearly equal and the V–V separation is 2.87 Å. Below 69°C, VO_2 transforms to the monoclinic variety in which the chains of cations sharing octahedral edges have alternating short, 2.62 Å, and long, 3.17 Å, separations creating a charge density wave. The VO_6 octahedra in the two forms display different distortions. In the tetragonal case the distance between the bridging oxygen atoms shortens in order to minimize the electrostatic repulsion between V^{4+} ions. The α ratio, the distance between bridging anions to

TABLE 3
Anisotropic Displacement Parameters

Atom	U_{11}	U_{22}	U_{33}	U_{12}	U_{13}	U_{23}
Ba(1)	0.0081(1)	0.0099(1)	0.0096(1)	0	0.0037(1)	0
Ba(2)	0.0153(1)	0.0209(1)	0.0139(1)	0	0.0098(1)	0
V(1)	0.0070(3)	0.0060(3)	0.0097(3)	0	0.0043(3)	0
V(2)	0.0074(3)	0.0087(3)	0.0064(3)	0	0.0018(2)	0
V(3)	0.0064(5)	0.0054(6)	0.0078(6)	−0.0013(4)	0.0021(5)	−0.0011(4)
O(1)	0.0167(11)	0.0088(9)	0.0117(10)	0.0019(8)	0.0026(10)	0.0017(8)
O(2)	0.0074(9)	0.0081(9)	0.0180(11)	−0.0009(7)	0.0051(9)	−0.0010(8)
O(3)	0.0348(25)	0.0276(21)	0.0311(24)	0	0.0278(22)	0
O(4)	0.0171(19)	0.0566(30)	0.0154(18)	0	0.0110(16)	0
O(5)	0.0102(15)	0.0166(16)	0.0155(16)	0	−0.0014(13)	0
O(6)	0.0090(14)	0.0125(14)	0.0107(14)	0	0.0036(12)	0
O(7)	0.0116(14)	0.0076(12)	0.0077(13)	0	0.0016(11)	0

Note. The anisotropic temperature factor is defined by $U = \exp(-2\pi^2[\Sigma i\Sigma jh_ih_ja_i^*a_j^*U_{ij}])$.

TABLE 4
Interatomic Distances (Å) and Selected Bond Angles (°) for $Ba_2V_3O_9$

Ba(1) Environment	Ba(2) Environment
Ba(1)–O(1) : 2.821(2)	Ba(2)–$O(1)^{iii}_{101}$: 2.726(3)
Ba(1)–$O(1)^{ii}$: 2.821(2)	Ba(2)–$O(1)^{iv}_{101}$: 2.726(3)
Ba(1)–$O(1)^{iii}_{100}$: 2.673(3)	Ba(2)–$O(2)^{iii}_{101}$: 2.785(3)
Ba(1)–$O(1)^{iv}_{100}$: 2.673(3)	Ba(2)–$O(2)^{iv}_{101}$: 2.785(3)
Ba(1)–$O(2)^{iii}_{101}$: 2.913(2)	Ba(2)–$O(4)^{i}_{101}$: 2.718(4)
Ba(1)–$O(2)^{iv}_{101}$: 2.913(2)	Ba(2)–(5) : 2.787(4)
Ba(1)–O(3) : 2.689(6)	Ba(2)–$O(7)^{i}_{101}$: 3.190(4)
Ba(1)–$O(5)^{iii}_{101}$: 3.079(1)	
Ba(1)–$O(5)^{iii}_{111}$: 3.079(1)	⟨Ba–O⟩ : 2.82(17)
Ba(1)–O(6) : 2.897(4)	
⟨Ba–O⟩ : 2.86(15)	
V(1) tetrahedron	**V(2) tetrahedron**
V(1)–O(2) : 1.763(3)	V(2)–O(1) : 1.693(2)
V(1)–$O(2)^{ii}$: 1.763(3)	V(2)–$O(1)^{ii}$: 1.693(2)
V(1)–O(3) : 1.660(6)	V(2)–O(4) : 1.650(6)
V(1)–O(5) : 1.669(3)	V(2)–O(7) : 1.847(3)
⟨V(1)–O⟩ : 1.71(6)	⟨V(2)–O⟩ : 1.72(9)
O(2)–V(1)–$O(2)^{ii}$: 112.1(3)	O(1)–V(2)–$O(1)^{ii}$: 105.9(3)
O(2)–V(1)–O(3) : 110.2(5) 2x	O(1)–V(2)–O(4) : 108.3(4) 2x
O(2)–V(1)–O(5) : 108.1(3) 2x	O(1)–V(2)–O(7) : 113.0(3) 2x
O(3)–V(1)–O(5) : 107.9(5)	O(4)–V(2)–O(7) : 108.2(4)
Average: 110(2)	Average: 109(2)
O–O lengths	O–O lengths
O(2)–$O(2)^{ii}$: 2.925(5)	O(1)–$O(1)^{ii}$: 2.703(5)
O(2)–O(3) : 2.808(6)	O(1)–O(4) : 2.710(5)
O(2)–O(5) : 2.779(3)	O(1)–O(7) : 2.952(3)
O(3)–O(5) : 2.692(7)	O(4)–O(7) : 2.834(6)
V(3) octahedron	
V(3)–O(2) : 1.999(3)	O(2)–V(3)–O(6) : 99.0(2)
V(3)–$O(2)^{iii}_{101}$: 1.981(3)	O(2)–V(3)–$O(6)^{iii}_{201}$: 88.79(2)
V(3)–O(6) : 1.686(3)	O(2)–V(3)–$O(7)^{i}_{101}$: 90.5(2)
V(3)–$O(6)^{iii}_{201}$: 2.240(3)	O(2)–V(3)–$O(7)^{iii}_{100}$: 86.9(2)
V(3)–$O(7)^{i}_{101}$: 1.985(3)	$O(2)^{iii}_{101}$–V(3)–O(6) : 96.9(3)
V(3)–$O(7)^{iii}_{100}$: 2.048(2)	$O(2)^{iii}_{101}$–V(3)–$O(6)^{iii}_{201}$: 83.2(2)
	$O(2)^{iii}_{101}$–V(3)–$O(7)^{i}_{101}$: 88.1(2)
⟨V(3)–O⟩ : 2.0(2)	$O(2)^{iii}_{101}$–V(3)–$O(7)^{iii}_{100}$: 89.2(2)
O–O lengths	O(6)–V(3)–$O(7)^{i}_{101}$: 89.8(3)
O(2)–O(6) : 2.180(4)	O(6)–V(3)–$O(7)^{iii}_{100}$: 105.8(1)
O(2)–$O(6)^{iii}_{201}$: 2.753(5)	$O(6)^{iii}_{201}$–V(3)–$O(7)^{i}_{101}$: 89.8(1)
O(2)–$O(7)^{i}_{101}$: 2.829(5)	$O(6)^{iii}_{201}$–V(3)–$O(7)^{iii}_{100}$: 74.5(2)
O(2)–$O(7)^{iii}_{100}$: 2.782(4)	
O(6)–$O(7)^{i}_{101}$: 2.601(5)	
O(6) : $O(7)^{iii}_{100}$: 2.987(1)	
V–V lengths	
V(3)–V(1) : 3.227(1)	
V(3)–$V(1)^{iii}$: 3.358(2)	
V(3)–V(2) : 3.583(1)	
V(3)–$V(2)^{iii}$: 3.3426(1)	
V(3)–V(3) : 3.007(1)	

Note. Symmetry codes: i: x, y, z; ii: x, 1/2 − y, z; iii: $\bar{x}$, $\bar{y}$, $\bar{z}$; vi: $\bar{x}$, 1/2 + y, $\bar{z}$. Subscripts denote atomic locations in translated unit cells.

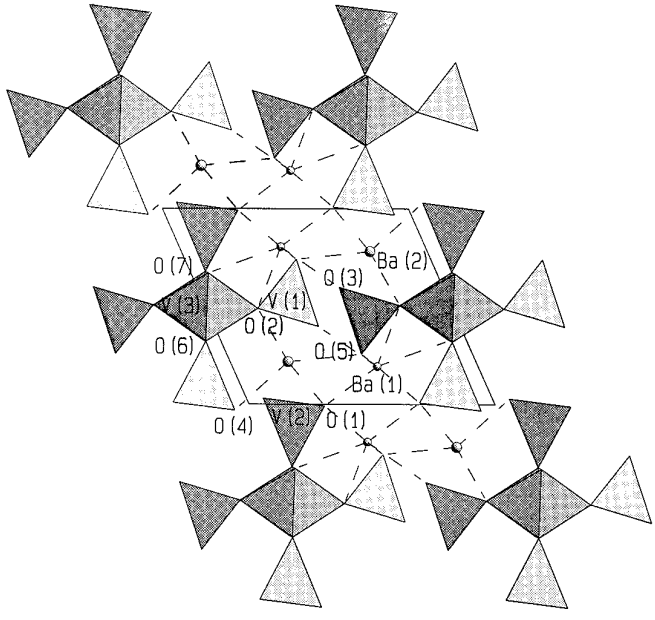

FIG. 1. The $Ba_2V_3O_9$ structure projected on (010).

the average of the remaining interanion separations along octahedral edges, is close to 0.9. In the monoclinic form, the bridging oxygen atoms are displaced from each other, allowing the formation of V–V metal bonds across the octahedral edge and α is 0.97 (21). In $Ba_2V_3O_9$ the bridging O(6)–O(7) bond is shortened and α is 0.92. Thus the structure is essentially ionic and no metal–metal bonds are present. However, V(3) is displaced from the center of the octahedron toward O(6) and the V(3)–O(6) distance, 1.686(3) Å, is characteristic of a double V=O bond. This distance is about 0.30 Å shorter than the four equatorial V–O bonds ranging from 1.981(3) to 2.048(2) Å. The V(3)–O(6) bond *trans* to the double bond is 2.240(3) Å.

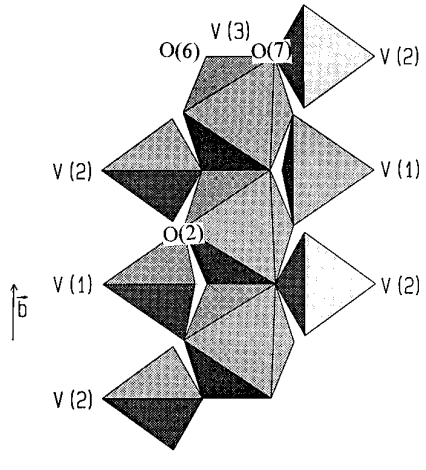

FIG. 2. The column $[V_3O_9]^{4-}_{\infty}$ in $Ba_2V_3O_9$.

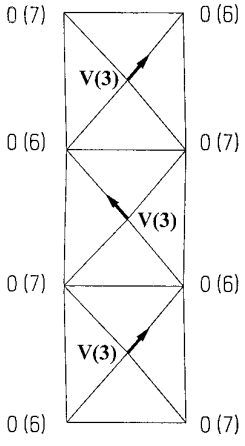

FIG. 3. The V(3) displacement within a single rutile-type chain in $Ba_2V_3O_9$.

The V(3) atom is disordered and occupies a site randomly displaced from the (0, 0, 1/2) octahedron center toward the two O(6) atoms. In one rutile-type chain two adjacent V(3) atoms need to be related by a 2_1 axis and the V(3) displacement is cooperative intrachain but not interchain, leading to a V(3)–V(3) distance of 3.007(1) Å (Fig. 3). If this is not the case it would lead to the unlikely configuration O=V=O. The long V–V distance doesn't allow vanadium t_{2g} orbitals to overlap leading to a localized electron system. Indeed, $Ba_2V_3O_9$ is an insulator between room temperature and 30 K. Random displacement of the V(3) atoms in the octahedra occurs among the columns. If V(3) were displaced toward the same O(6) atom for all the columns the space group becomes $P2_1$. Refinement in $P2_1$ led to greater values of $R = 0.036$ and $R_w = 0.044$ in spite of a greater number of refined parameters, 127. This model can be safely rejected on the basis of the Hamilton ratio test $R_{127,1435,0.005} \approx 1.05$ as compared to the observed ratio 1.57 (18).

The V(1)O4 and V(2)O4 tetrahedra share corners with the VO6 octahedra. The V(1)O4 tetrahedra are bidentate, bridging two adjacent VO6 octahedra through O(2). The V(2)O4 tetrahedra share O(7) with the octahedra. The O(6) oxygen atom of the vanadyl bond is unshared. Within tetrahedra the V–O distances to oxygen atoms shared with VO6 octahedra are longer than the V–O distances to unshared oxygen atoms (Table 4). The average V–O bond lengths for V(1) and V(2) atoms, 1.71(6) and 1.72(9) Å, respectively, are in good agreement with the sum of ionic radii of V^{5+} in C.N.IV and O^{2-}, 1.73 Å, whereas the average V(3)–O bond length of 2.0 Å agrees with $r[V^{4+}$ (C.N.VI)] + $r(O^{2-}) = 1.96$ Å (22). These results strongly suggest that V(1) and V(2) are V^{5+} and V(3) is V^{4+}. Moreover bond-length and bond-strength calculations using the method of Brown and Shannon (23) and the data of Brown and Altermatt (24) give bond valence sums for V(1) = 5.14, V(2) = 5.09, and V(3) = 3.81, indicating that V(1) and V(2) are pentavalent and that V(3) is tetravalent. Based on these results this mixed valence vanadium oxide is a vanadyl(IV) vanadate and the chemical formula can be written as $Ba_2(V^{4+}O)(V^{5+}O_4)_2$.

Ba(1) is coordinated by 10 oxygen atoms with an average Ba–O distance of 2.86(15) Å while Ba(2) is coordinated by six oxygen atoms forming a distorted octahedron with an average Ba–O distance 2.75(3) Å with a seventh oxygen atom at 3.190(4) Å (Fig. 4). The bond valence sums for Ba(1) and Ba(2) are 2.32 and 1.78, respectively, and the underbonding for Ba(2) may be the cause of the larger value of the displacement parameter.

$Ba_2(VO)(VO_4)_2$ is the first example of a vanadium compound containing isolated rutile-type chains linked to tetrahedra. In VO_2, the rutile chains are connected to each other by corner sharing (Fig. 5a); in hollandite and hollandite-related compounds the rutile chains share edges to form double strings and the double strings are connected at their corners to form a $[V_8O_{16}]$ framework structure (Fig. 5b). In the hollandite-related structure $Pb_{1.32}V_{8.35}O_{16.70}$, extra VO_4 tetrahedra occupy the large tunnels of the $[V_8O_{16}]$ framework and are attached to the VO_6 octahedral framework (1). Isolated rutile chains are found with metal ions other than vanadium in compounds of formula A_2MO_4, e.g., in Pb_2PtO_4 (25), in which the rutile chains are connected only by A^{2+} ions (Fig. 5c).

Different types of one-dimensional chains separated by Ba^{2+} cations are also found in the vanadyl phosphate compounds $Ba_2(VO)(PO_4)_2 \cdot H_2O$ (11) and $Ba_8(VO)_6(HPO_4)_{11} \cdot 3H_2O$ (14). In the former, vanadium atoms are disordered on a site displaced from the octahedron center to an apex oxygen forming a short V=O bond (1.580 Å) and a long *trans* V–O bond. Although the two oxygen atoms of the O=V–O moiety are crystallographically related, they represent either an O=V oxygen or an oxygen of a water molecule. The latter compound exhibits two types of one-dimensional chains involving independent V(1) and V(2) octahedral atoms. The $V(1)O_6$ octahedron doesn't show evidence of a short V=O bond but the V(1) site is believed to be an average of superimposed O–V=O

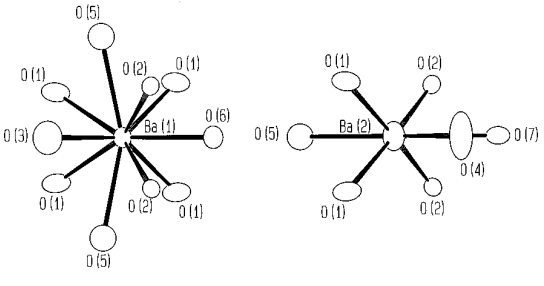

FIG. 4. The oxygen environment around Ba(1) and Ba(2).

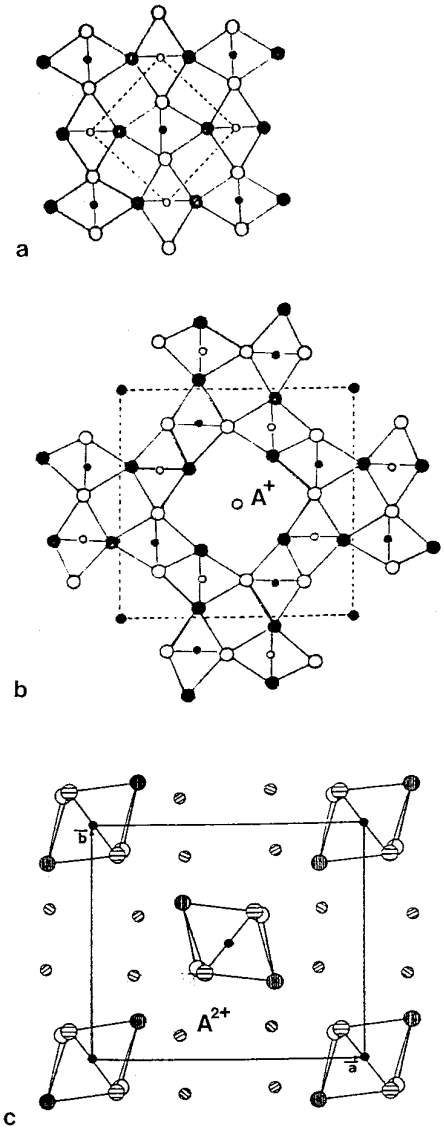

FIG. 5. Rutile-type chains (a) connected at corners, e.g., VO_2, (b) edge-shared in a hollandite framework, and (c) isolated in A_2MO_4 compounds.

and O=V–O configurations. In the $V(2)O_6$ octahedron a short vanadyl bond (1.596 Å) is observed. Recently, several barium vanadyl-arsenates, -phosphates, and -hydrogenophosphates have been studied and they exhibit various frameworks; e.g., $Ba(VO)_2(AsO_4)_2$ and its isomorph $Sr(VO)_2(AsO_4)_2$ consist of one-dimensional cationic tunnels, the framework being composed, as in $Ba_2V_3O_9$, of edge sharing VO_6 octahedra, but in these two isostructural compounds only one O–O edge is shared between two VO_6 octahedra forming V_2O_{10} dimers with two intradimer V=O bonds of 1.59 Å (13). An example of a two-dimensional structure containing V=O bonds, 1.605 Å, is provided by $Ba(VO)(PO_4)(H_2PO_4)\cdot H_2O$ in which $V^{4+}O_6$ octahedra and PO_4 groups are linked by corners into anionic layers (12). Finally, two types of tetravalent vanadium V=O groups are present in the three-dimensional framework of $Ba(VO)_2(PO_4)_2$ with bond lengths 1.603 and 1.611 Å (10).

It is important to emphasize that the octahedral V^{4+}=O bond in $Ba(VO)(VO_4)_2$, 1.686(3) Å, is significantly longer than in the previously mentioned barium vanadyl compounds. The same effect is also observed when comparisons are made with the square pyramidal vanadyl(IV) ion present in mixed valence vanadium oxides such as $Cs_2V_5O_{13}$ (26) (V=O = 1.607 Å), $K_2V_3O_8$ (27) (V=O = 1.582 Å), and the recently published intercalated vanadyl vanadate ($V^{4+}O(V^{5+}O_4)\cdot 0.5[CH_3N_2H_{12}]$ (28). In this compound, two $V^{4+}O_5$ vanadyl square pyramids share an edge to form V_2O_8 dimers similar to those observed in compounds derived from carnotite such as $(Na_{1-x}K_x)UO_2(V_2O_8)$ in which the V=O bond distances are 1.579 Å (29). Many other new barium vanadium oxides, phosphates, or hydrogenophosphates such as $Ba(VO_2)PO_4$ (30), $Ba_8V_7O_{22}$ (8), and $Ba[V_2(HPO_4)_4]\cdot H_2O$ (15) have been recently synthesized, notably by hydrothermal synthesis, but they don't exhibit short V=O vanadyl bonds.

Infrared Spectroscopy

The IR data for $Ba_2V_3O_9$ show typical bands associated with orthovanate V–O and vanadyl V=O resonances (Fig. 6). The classical vibrations of the tetrahedral VO_4^{3-} ion, $\nu 1$, $\nu 3$, and $\nu 4$, are observed. They can be empirically assigned on the basis of previous results on orthovanadate compounds (31–34). Thus, the 944–838 cm^{-1} and the 490–400 cm^{-1} multiplets are attributed to asymmetric stretching, $\nu 3$, and symmetric bending, $\nu 4$, vibrations, respectively. The ratio of the average intensity of the two-multicomponent peaks to the $\nu 1$ sharp band intensity has been found to be close to 1 for orthovanadates with the apatite structure (34). Such considerations applied to our case indicate a 705 cm^{-1} symmetric stretching $\nu 1$ vibration. The remaining sharp band which appears at 770 cm^{-1} is assigned to the V=O stretching vibration and is lower in energy with respect to other vanadyl compounds (10, 14, 35).

Magnetic Measurements

Figure 7 shows the plot of χ and χ^{-1} vs T. The reversibility of the ZFC and FC data indicate that the magnetic susceptibility is not history dependent. From room temperature to about 100 K, the inverse susceptibility can be modeled by the Curie–Weiss relationship, $\chi^{-1} = (T - T_c)/C$. The diamagnetic corrections were neglected. A least squares fit yielded C = 0.512 emu K/mol Oe and T_c = −132.5 K. The calculated value μ_{eff} = 2.0 μ_B per formula unit is slightly higher than the expected value of 1.73 for a V^{4+} spin-only ion and is due to a spin-orbital contribution.

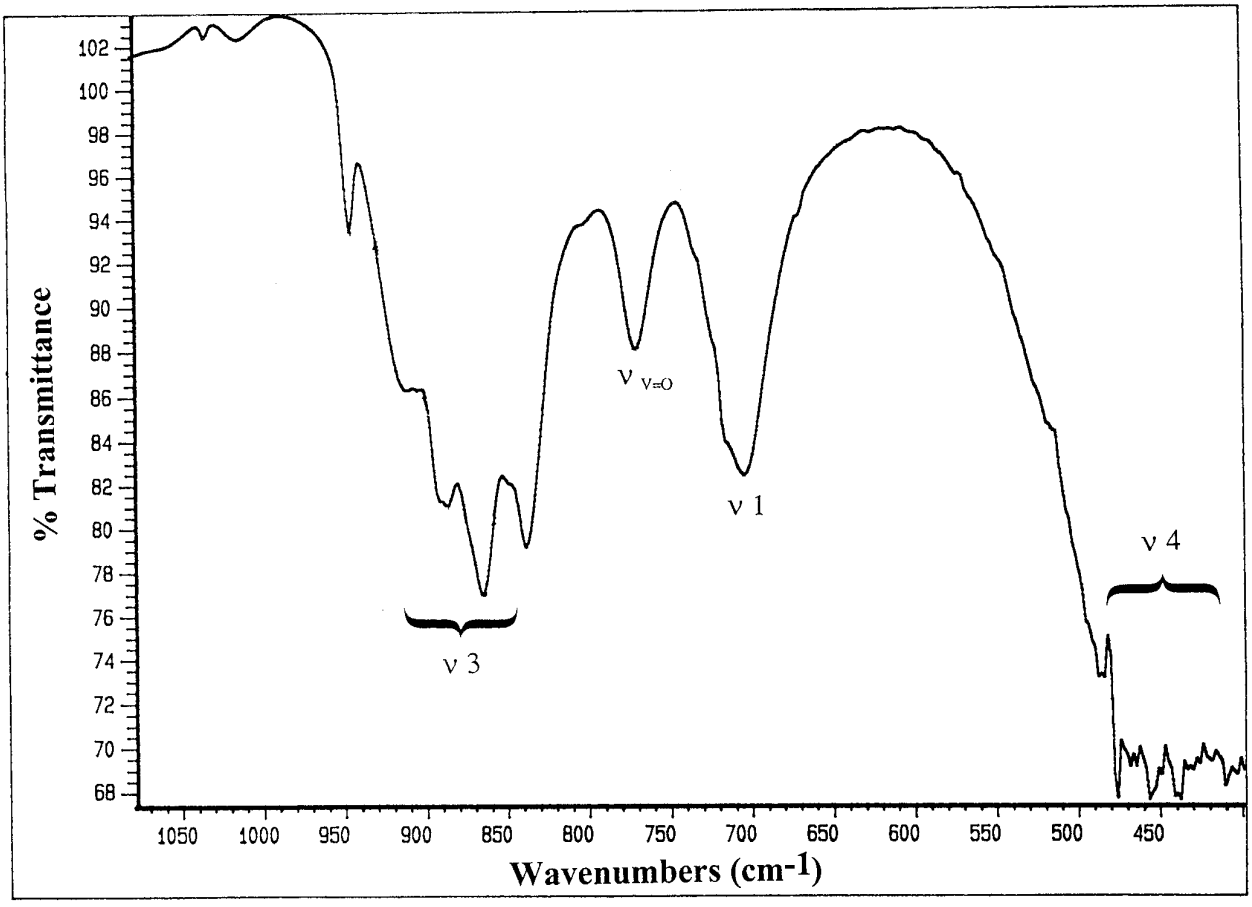

FIG. 6. Infrared spectrum of $Ba_2V_3O_9$.

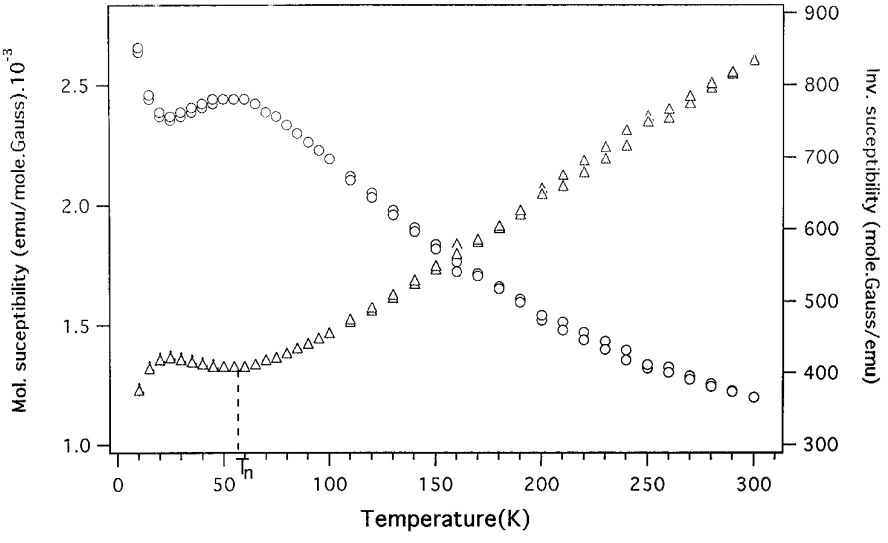

FIG. 7. Temperature dependencies of magnetic susceptibility (circles) and inverse susceptibility (triangles) of a polycrystalline $Ba_2V_3O_9$ specimen.

The compound is an antiferromagnet with $T_N = -58$ K. The change at about 20 K could indicate the presence of a small amount of a paramagnetic impurity. On the other hand it might be due to a ferromagnetic exchange coupling that causes a canted-spin arrangement of the V^{4+} ions along the rutile chains (Fig. 3). Three possible interactions can induce this kind of noncolinear spin arrangement in $Ba_2V_3O_9$:

1. Metal–metal double exchange through $2p^6$ oxygen orbitals, but this is unlikely because of the single 4+ valence of the vanadium ions along the *b* axis.

2. Dzyaloshinski–Moriya interactions (36, 37) are not possible because of the centrosymmetric space group.

3. The presence of magnetic anisotropy is the most likely explanation for the spin canting away from the antiferromagnetic spin alignment. Indeed, the existence of a double vanadyl bond between octahedral V^{4+} and a bridging oxygen splits the $3t_{2g}$ low energy orbitals into one with lower energy occupied by the d^1 electron and two empty orbitals at slightly higher energy. Thus overlapping $2p^6$ orbitals generate a strong anisotropy in the octahedral crystal field tilting the antiferromagnetically aligned spins along the zigzag vanadyl chains. Similar behavior has been observed in $Ba_8(VO)_6(HPO_4)_{11} \cdot 3H_2O$ but cannot be justified in the same way because of the long V–O–P–O–V superexchange between V^{4+} (14).

SUMMARY

The crystal structure of a previously reported compound, $Ba_2V_3O_9$, was determined and its IR spectrum and magnetic susceptibility were investigated. The compound is a vanadyl vanadate, $Ba_2(VO)(VO_4)_2$. Edge sharing octahedra have attached to them tetrahedra to form a free standing column of composition $V_3O_9^{4-}$. The octahedra are occupied by V^{4+} that are slightly displaced from the octahedron center to form a V=O double bond to one oxygen and the tetrahedra are occupied by V^{5+}. The IR spectrum is consistent with the presence of a vandyl group. The magnetic susceptibility shows that the material has Curie–Weiss behavior between 100 K and room temperature and a $\mu_{eff} = 2\,\mu_B$ with T_N about 58 K. At about 20 K a ferromagnetic component becomes important to give rise to spin canting. The crystal structures of $Sr_2V_3O_9$ and isostructural $Pb_2V_3O_9$ are now under investigation.

ACKNOWLEDGMENTS

HS and OM gratefully acknowledge the support for this research by the R. A. Welch Foundation, Houston, Texas.

REFERENCES

1. O. Mentre and F. Abraham, *J. Solid State Chem.,* accepted for publication.
2. M. E. De Roy, J. P. Besse, and R. Chevalier, *J. Solid State Chem.* **67,** 185 (1987).
3. Y. Kanke, E. Takayama-Muromachi, K. Kato, and Y. Matsui, *J. Solid State Chem.* **89,** 130 (1990).
4. Y. Kanke, F. Izumi, E. Takayama-Muromachi, K. Kato, T. Kamiyama, and H. Asano, *J. Solid State Chem.* **92,** 261 (1991).
5. Y. Kanke, E. Takayama-Muromachi, K. Kato, and K. Kosuda, *J. Solid State Chem.* **113,** 125 (1994).
6. J. C. Bouloux, J. Galy, and P. Hagenmuller, *Rev. Chim. Miner.* **11,** 48 (1974).
7. Y. Kanke, E. Takayama-Muromachi, K. Kato, and K. Kosuda, *J. Solid State Chem.* **115,** 88 (1995).
8. G. Liu and J. E. Greedan, *J. Solid State Chem.* **108,** 371 (1994).
9. L. Benhamada, A. Grandin, M. M. Borel, A. Leclaire, and B. Raveau, *Acta Crystallogr. C* **47,** 2437 (1991).
10. A. Grandin, J. Chardon, M. M. Borel, A. Leclaire, and B. Raveau, *J. Solid State Chem.* **99,** 297 (1992).
11. W. T. A. Harrison, S. C. Lim, J. T. Vaughey, A. J. Jacobson, D. P. Goshorn, and J. W. Johnson, *J. Solid State Chem.* **113,** 444 (1994).
12. W. T. A. Harrison, S. C. Lim, L. L. Dussack, A. J. Jacobson, D. P. Goshorn, and J. W. Johnson, *J. Solid State Chem.* **118,** 241 (1995).
13. S. Wang and C. Cheng, *J. Solid State Chem.* **109,** 277 (1994).
14. W. T. A. Harrison, S. C. Lim, J. T. Vaughey, A. J. Jacobson, D. P. Goshorn, and J. W. Johnson, *J. Solid State Chem.* **116,** 77 (1995).
15. Z. Wang, R. C. Haushalter, M. E. Thompson, and J. Zubieta, *Mater. Chem. and Phys.* **35,** 205 (1993).
16. International Centre for Diffraction Data, JCPDS—ICDD, Newton Square, Pennsylvania, Pattern 26-1039.
17. J. De Meulenaer and H. Tompa, *Acta Crystallogr.* **19,** 1014 (1965).
18. International Tables for X-ray Crystallography, Vol. IV. Kynoch Press, Birmingham, 1974.
19. D. T. Cromer and D. Liberman, *J. Chem. Phys.* **53,** 1891 (1970).
20. C. T. Prewitt, SFLS-5, Report ORN-L-TM 305. Oak Ridge National Laboratory, Oak Ridge, Tennessee, 1966.
21. D. B. Rogers, R. D. Shannon, A. W. Sleight, and J. L. Gillson, *Inorg. Chem.* **8,** 841 (1969).
22. R. D. Shannon, *Acta Crystallogr. A* **32,** 751 (1976).
23. I. D. Brown and R. D. Shannon, *Acta Crystallogr. A* **29,** 266 (1973).
24. I. D. Brown and D. Altermatt, *Acta Crystallogr. B* **41,** 244 (1985).
25. N. Bettahar, P. Conflant, F. Abraham, and D. Thomas, *J. Solid State Chem.* **67,** 85 (1987).
26. K. Waltersson and B. Forslund, *Acta Crystallogr. B* **33,** 784 (1977).
27. J. Galy and A. Carpy, *Acta Crystallogr. B* **31,** 1794 (1975).
28. D. Riou and G. Ferey, *J. Solid State Chem.* **120,** 137 (1995).
29. F. Abraham, C. Dion, and M. Saadi, *J. Mater. Chem.* **3,** 459 (1993).
30. H. Y. Kang, S. L. Wang, and K. H. Lii, *Acta Crystallogr. C* **48,** 975 (1992).
31. F. Gonzales-Vilchez and W. P. Griffith, *J. Chem. Soc. Dalton Trans.* 1416, (1972).
32. N. Weinstock, M. Schulze, and A. Muller, *J. Chem. Phys.* **59,** 5063 (1973).
33. E. J. Baran and P. J. Aymonino, *Z. Anorg. Allg. Chem.* **390,** 77 (1972).
34. J. W. Johnson, A. J. Jacobson, J. F. Brody, and S. M. Rich, *Inorg. Chem.* **21,** 3821 (1982).
35. G. Villeneuve, A. Erragh, D. Beltran, M. Drillon, and P. Hagenmuller, *Mater. Res. Bull.* **21,** 621 (1968).
36. I. Dzyaloshinski, *J. Phys. Chem. Solids* **4,** 241 (1958).
37. T. Moriya, *in* "Magnetism" (G. T. Rado and H. Suhl, Eds.), Vol. I, Chap. 3. Academic Press, New York, 1963.